

MODIFIED D-GLUCOFURANOSE COMPUTATIONALLY SCREENING FOR INHIBITOR OF BREAST CANCER AND TRIPLE BREAST CANCER: CHEMICAL DESCRIPTOR, MOLECULAR DOCKING, MOLECULAR DYNAMICS AND QSAR

AJOY KUMER ^{1,2*}, UNESCO CHAKMA ³, AKHEL CHANDRO ⁴, DEBASHIS HOWLADER ³, SHOPNIL AKASH ⁵, MD. ELEAS KOBIR ⁶, TOMAL HOSSAIN ³ AND MOHAMMED M. MATIN ⁷

¹Laboratory of Computational Research for Drug Design and Material Science, Department of Chemistry, European University of Bangladesh, Gabtoli, Dhaka-1216, Bangladesh..

²Department of Chemistry, Bangladesh University of Engineering and Technology, Dhaka-1000, Bangladesh.

³Department of Electrical and Electronics Engineering, European University of Bangladesh, Gabtoli, Dhaka-1216, Bangladesh.

⁴Faculty of Animal Science & Veterinary Medicine, Department of Poultry Science, Sher-e-Bangla Agricultural University, Dhaka, Bangladesh.

⁵Department of Pharmacy, Daffodil International University, Sukrabad, Dhaka-1207, Bangladesh.

⁶Department of Pharmacy, Atish Dipankar University of Science & Technology, Uttara, Dhaka-1230, Bangladesh.

⁷Bioorganic and Medicinal Chemistry Laboratory, Department of Chemistry, Faculty of Science, University of Chittagong, Chittagong, 4331, Bangladesh.

ABSTRACT

Drug discovery and the process of new drug design have been formulated much easier in the past two decades by introducing, proliferation of combined physical, biochemical process from computing capabilities and computational approaches. Since the breast cancer is one of the life-threatening problems globally, no effective prescription is still now invented or not available in the market or medical treatment. Although the few number of drugs is just touched on the market, the remedy has consisted of severe side effects and low efficiency. Regarding that fact, the D-glucufuranose and its derivatives have been designed by the quantum calculation, molecular docking, ADMET and SAR analysis. For molecular docking, the cancer protease (3hb5) and triple-negative breast cancer protease (4pv5) are selected for study whereas the binding affinity of cancer protease (3hb5) is found at ranging from -6.20 to -10.40 kcal/mol, and it is slightly lower than triple-negative breast cancer protease (4pv5). Next, the molecular dynamic has performed to make the validation of docking complex. In our forthcoming study, it has shown that the 03, 05, and 08 compounds could be considered the potential drug comparison with standard drug. These three drugs completed all the criteria, including high binding energy, non-toxic, non-carcinogenic, and highly soluble in biological system.

Keywords: Triple-negative breast cancer, Breast cancer, DFT, HOMO-LUMO, Docking, Molecular dynamics, and ADMET.

1. INTRODUCTION

Cancer is one of the significant life-threatening problems globally after coronary heart disease, and it has been seemed to be the second-largest incidence of mortality in our globe (1-3). Cancer occurs when the immune system is not correctly functionalized, or the number of cells is started into too large spontaneously cell division or abnormal cell division (4). In addition, different conditions can as well lead to the development of cancer in the human body caused by the rate of DNA and RNA alterations, an unhealthy environment (radioactive materials and other substances) (5), inadequate nutrition, unhealthy cell environment (6). Persons are genetically susceptible to abnormalities (7), people over 80 years (8), a category of illnesses, and terminating in a lump (9, 10). Although several types of cancer have been seen, it has increased by 29 percent among females worldwide compared to all other cancer diagnoses (11). BC may also occur due to genetic factors (12) and non-genetic risk factors (13), such as hormonal causes (14), overweight or obesity (15, 16), and not getting enough physical activity (17, 18).

Based on the report of the American Institute of Cancer Research (2018), Belgium, 113.2 Luxembourg 109.3 Netherlands 105.9 France (metropolitan) 99.1 New Caledonia (France) 98 Lebanon 97.6 Australia 94.5 UK 93.6 Italy 92.8 New Zealand 92.6 people have been faced breast cancer in Age-standardized rate per 100,000. Belgium has the most significant percentage of females who have been reported of breast cancer disease (19). There are many proteases for breast cancer (PDB ID: 3hb5); Two-dimensional crystal structural analysis of a potential 17-HSD type I inhibitor and a promising lead chemical for breast cancer treatment. Hydrogen bonds and hydrophobic contacts are among many interactions involving E2B and the enzyme, as well as π - π interaction (20). Secondly, triple-negative breast cancer protease (PDB ID: 4pv5); the over expression of Glyoxal I (GLOI), which would be a glutathione (GSH)-dependent enzyme, seems associated with chemotherapy drug susceptibility (21).

Although breast cancer is spreading at a tremendous rate among females, many people are dying continuously. So far, no effective drug for breast cancer has not been possible to discover. So, the computational method has been chosen to design new and effective anticancer drugs from the D-glucufuranose by its modification. It is a well-known fact that finding an effective drug takes a lot of time and huge cost -an average of 10–15 years required and costs around \$800

million, which is highly expensive (22, 23). But with the help of the newly developed computational chemistry method, it has been possible to design an effective drug, and check all the pharmacokinetic parameters of the drug in a concise time, such as pass prediction, docking, molecular dynamics, and ADMET easily (24). On the other hand, the D-glucufuranose and its derivative have already been identified as a potential compound by many renowned researchers (25) for the treatment as an antifungal (25) antibacterial, antiviral (26-29), and anticancer activity (30). Since D-glucufuranose and its derivatives have already been found to have potential as antimicrobial and anticancer before (27, 29, 31, 32), this is why derivatives of this compound have been taken and performed different types of computational studies. Firstly, molecular docking investigation was conducted, and the docking score has been reported higher compared to the standard range. Then, it was thought that this drug could act as an anticancer activity through the computational approaches.

2. COMPUTATIONAL DETAILS

2.1 Optimization of molecules

For geometry optimization, the material studio was used to calculate chemical reactivity indicators using B3LYP, DFT method of DMol3 code from Material Studio 08 version (33-35). This method has been utilized to get an exact result. Highly precise result is obtained from DMol3 code. The B3LYP functional and basis set (DND) was set up properly due to the presence of the electronegative atom, oxygen. After geometric optimization, molecular orbitals were analyzed with levels of diagrams, HOMO and LUMO. After appropriately performed optimization, these optimized lead compounds were exported as pdb files for further computational investigation, such as molecular docking, molecular dynamic, and ADMET.

2.2 PASS prediction

The pass prediction data (Pa>Pi value) has been obtained from the online pass website "<http://way2drug.com/PassOnline/predict.php>," which is the most reliable and valuable website to predict molecules. Specifically, the antiviral, antifungal, anticancer, antibacterial, and antibiotic properties of Pa> Pi value were evaluated. This value is crucial for investigating and assessing newly drug candidate molecules' therapeutic and biological potency (36).

*Corresponding author email: kumarajoy.cu@gmail.com

2.3 Method for molecular docking

The three-dimensional structure of HER2-positive breast cancer tests positive for a protein called human epidermal growth factor receptor 2 (HER2), which enhances the growth of cancer cells. It was found in Protein Data Bank (PDB) with breast cancer protease, ID: (3hb5); and triple-negative breast cancer protease (4pv5), following link <https://www.rcsb.org/>, which is designated structural unit of breast cancer in the human body carrying with genetically properties. The obtained protein from PDB was viewed using the PyMol software version using PyMolV2.3 (<https://pymol.org/2/>) (37). To get the fresh protein, all water molecules and unexpected ligands or heteroatoms were removed and stored as PDB files. Drug PDB and protein files were uploaded to PyRx Virtual Screening Tools (38) for molecular docking as the auto dock vina. Finally, the docked complex was taken into the Discovery Studio version 2017 for viewing and analyzing the result (39).

2.4 Molecular Dynamics

Molecular dynamics (MD) is a tool used to study nuclear orientations where a single point model is replaced by a dynamic model, and the nuclear system is forced to be dynamic. The NAMD application has been applied to conduct the MD simulations on very high configuration desktops in live views or batch mode (40). MD simulation was enthusiastic to under the docking results gained for the best drugs and HER2-positive breast cancer protein up to 100 ns for holo-form (drug-protein) applying AMBER14 force field (41). The whole framework was equilibrated using 0.9 percent NaCl at 298 K heat in a water solution. At the simulation time, a cube was disseminated within 20 Å each side of the process and periodic boundary situation and was analyzed using RMSD and RMSF by VMD software.

2.5 Determination of the Lipinski rule and Drug likeness

The Lipinski rule of five assists in categorizing drug-like and non-drug-like compounds (42, 43). When it comes to structural characteristics of compounds, drug-likeness criteria have been employed to calculate a molecule's drug-like features more quickly (44). The primary focus on Lipinski five Rule is to determine (Hydrogen bond acceptor, Hydrogen bond donor, TPSA, Bioavailability Score, etc.), and it has been obtained by utilizing of SwissADME <http://www.swissadme.ch/index.php> free website (45) (Swiss Institute of Bioinformatics, Switzerland) (46).

2.6 Determination of the data of ADMET

An essential part of drug discovery is determining DMPK (drug metabolism and Pharmacokinetics) research, which is described to as ADMET (absorption, distribution, metabolism, elimination, toxicity) research. ADMET features were completed using the online database ADMETSAR, <http://lmmd.ecust.edu.cn/admetsar2>, the most trustworthy and reliable database for predicting the ADMET parameters (47-49).

2.7 Determination of the QSAR and PIC₅₀

QSAR is a quantum chemistry method that has been widely utilized to estimate the bioactivity of substances based on their molecular structure as a technique for forecasting medication efficacy in new drug discovery and development (50). QSAR and pIC₅₀ values were calculated with the help of the Chemdesk website and a standard equation is known as Multiple linear regression (MLR). From this free database of chemdesk, the required data (including Chiv5, MRVSA9, PEOEVSA5) has been collected then, develop an Excel sheet with Multiple linear regression (MLR), and the calculation of QSAR and PIC₅₀ has been completed for the reported Ligand (51). Particularly, describe the data, Chiv5 molecular connectivity, bcutm1 means burden descriptors, MRVSA9, MRVSA6 and PEOEVSA5 are MOE type descriptors; GATSV4 indicate autocorrelation descriptors, and the last two-parameter J and diametert suggested topological descriptors of drug molecules or biological compounds (51).

3. RESULTS AND DISCUSSIONS

3.1 Chemistry

D-glucufuranose and its analogs are extremely prevalent carbohydrate-containing molecules in the category of glucose of carbohydrate, and they exhibit both anticancer and antimicrobial effects. This is why they've been referred to the computational studying against breast cancer. The most likely objective of this research is to see what happens to anticancer activity when the side chains of D-glucufuranose molecules are modified. Figure 1 shows that the oxygen group and alkylating chain have been substituted by a -OH in the parent D-glucufuranose. Secondly, by introducing aromatic or benzene rings to the parent D-glucufuranose, the -OH has been replaced.

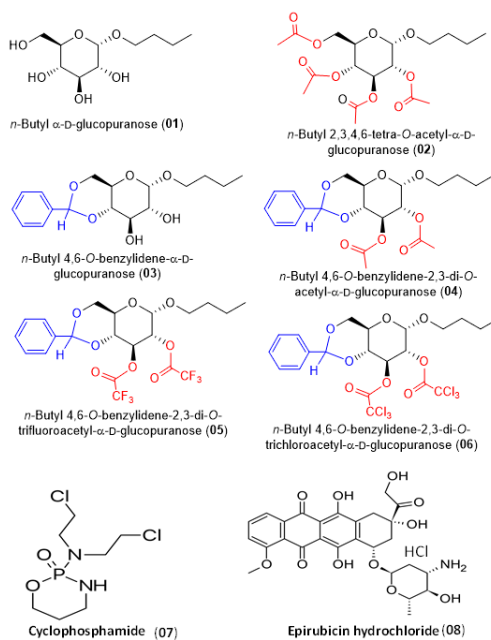


Figure 1. Molecular structure of D-glucufuranose and its derivative.

3.2 Optimized structure

To find a promising therapeutic candidate for clinical testing, structure-based drug discovery involves designing and optimizing chemical structures. After establishing an initial lead molecule, optimization has been performed to

generate an effective drug candidate (52). It relies upon understanding the drug's three-dimensional structure and how its form and charges induce it to interact with its biological target, eventually generating a therapeutic effect (53). The optimized structure is displayed in Figure 2.

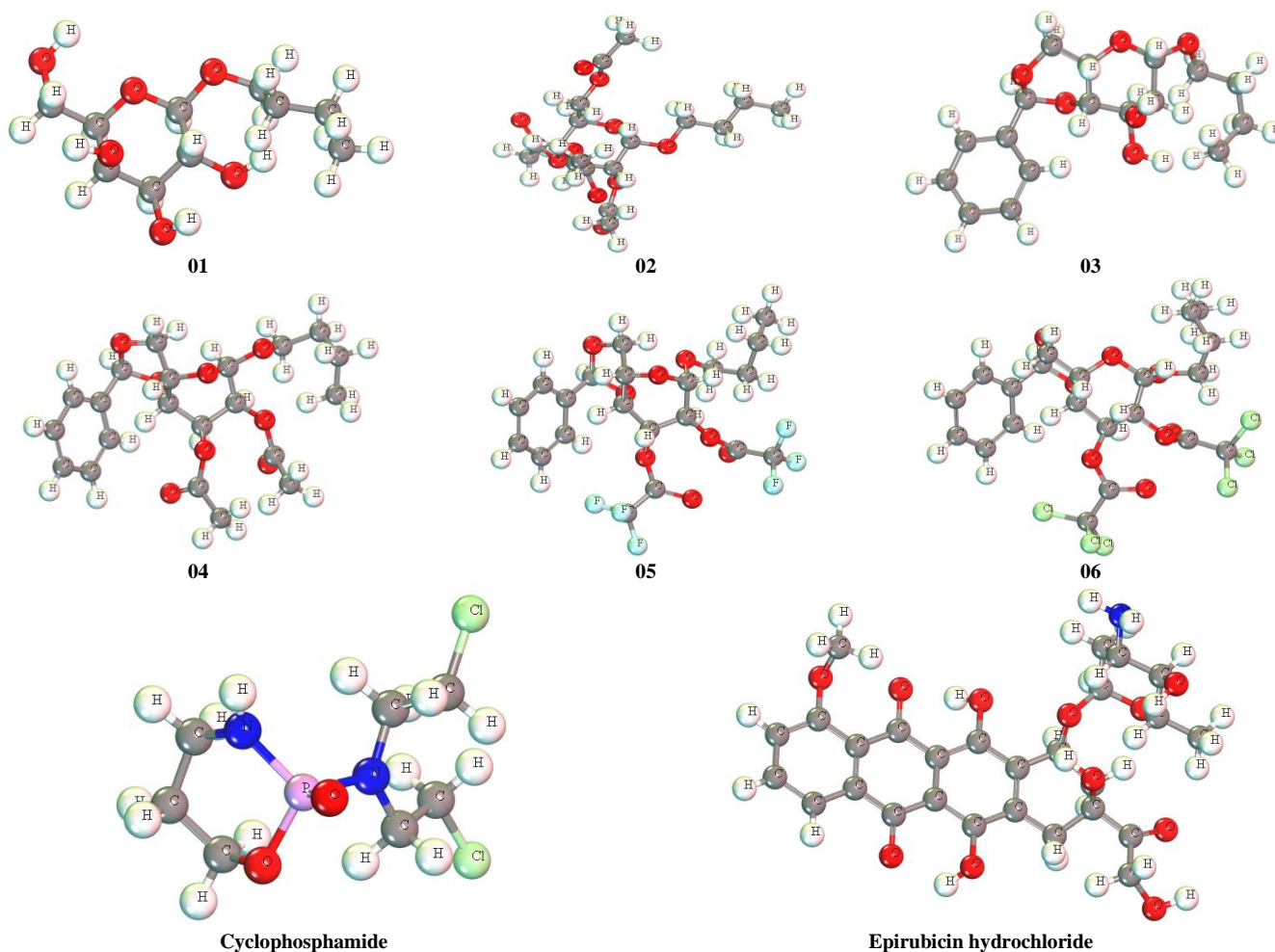


Figure 2. Optimized structure of D-glucufuranose and its derivatives.

3.3 HOMO, LUMO, and chemical reactivity descriptors

Table 1 shows the ϵ LUMO, ϵ HOMO, and ΔE gaps, chemical potential (μ), electronegativity (χ), stiffness (η), softness and electrophilicity (ω) of the drugs. These data have been calculated by utilizing B3LYP functional, leading to better geometry optimization results (54). The HOMO-LUMO energy gap determines the molecules' chemical sensitivity, and a large HOMO-LUMO gap refers to low chemical stability with high dynamics (55). The most fundamental distinction respectively HOMO and LUMO is that HOMO donates electrons, where LUMO receives electrons. Molecular interaction (HOMO/LUMO) predicts which molecules should have unusually high HOMOs and abnormally low LUMOs ultimately recognize the functional groups and indicate which functional groups are reacted or interacted with each other.

Table 1. Frontier molecular orbitals and reactivity descriptor analysis.

	ϵ LUMO, eV	ϵ HOMO, eV	ϵ HOMO- ϵ LUMO gap, eV	Ionization potential (I), eV	Electron affinity (A), eV	Chemical potential (μ), eV	Hardness (η), eV	Electrons activity (χ), eV	Electrophilicity (ω), eV	Softness (S), eV
01	-1.309	-10.469	9.079	10.469	1.309	-5.889	4.580	5.889	3.786	0.218
02	-0.787	-10.567	9.780	10.567	0.787	-5.677	4.890	5.677	3.295	0.204
03	-0.175	-8.626	8.451	8.626	0.175	-4.4005	4.225	4.400	2.291	0.236
04	-0.719	-8.614	7.895	8.614	0.719	-4.6665	3.947	4.666	2.758	0.253
05	-1.823	-8.990	7.167	8.99	1.823	-5.4065	3.583	5.406	4.078	0.279
06	-1.450	-9.094	7.644	9.094	1.450	-5.272	3.822	5.272	3.636	0.261
07	-1.390	-9.921	8.531	9.921	1.390	-5.6555	4.265	5.655	3.749	0.234
08	-2.923	-9.094	6.171	9.094	2.923	-6.0085	3.085	6.008	5.850	0.324

The orbitals that contain electrons are the highest in HOMO energy, and those that do not have electrons are the lowest in the LUMO energy (56-63).

From table 1, it is observed that the HOMO-LUMO gap is about 6.171 to 9.780 eV for all tested drugs, while 05 and 08 show the lowest energy gap and have the highest softness value. However, 05 and 08 show better performance than others with a lower energy gap. The chemical reactivity and active sites of the molecules were determined by frontier molecular orbital (FMO), where the protein can be banded, and the lower magnitude of energy gap contributes to form an interaction with HER2-positive breast cancer cell protein with drugs. The HOMO-LUMO gap is dynamically higher, reduces the molecules' stability, and will quickly dissolve it, resulting in faster actions. The value of HOMO-LUMO difference, softness, electron activity of Table 1 clarifies that all the drugs can capable prevent the spread of breast cancer cells in the human body.

3.4 Frontier molecular orbital: HOMO and LUMO

In terms of physicochemical parameters, the HOMO and the lowest LUMO orbitals have such a significant role, as well as protein interaction has enormous biological importance (64-70). The orbital geometries determined by DFT, HOMO orbitals have electron denser regions, whereas LUMO orbitals have been

considered electron-deficient regions. In Figure 3, LUMO is typically present where the positive charge has been placed, and the HOMO is present where the negative charge is placed. The deep green highlights the positive portion in HOMO, and the deep red hue has marked negative node. The lightest shade of maroon symbolizes the orbital's positive side of LUMO, while yellow indicates its negative side of LUMO.

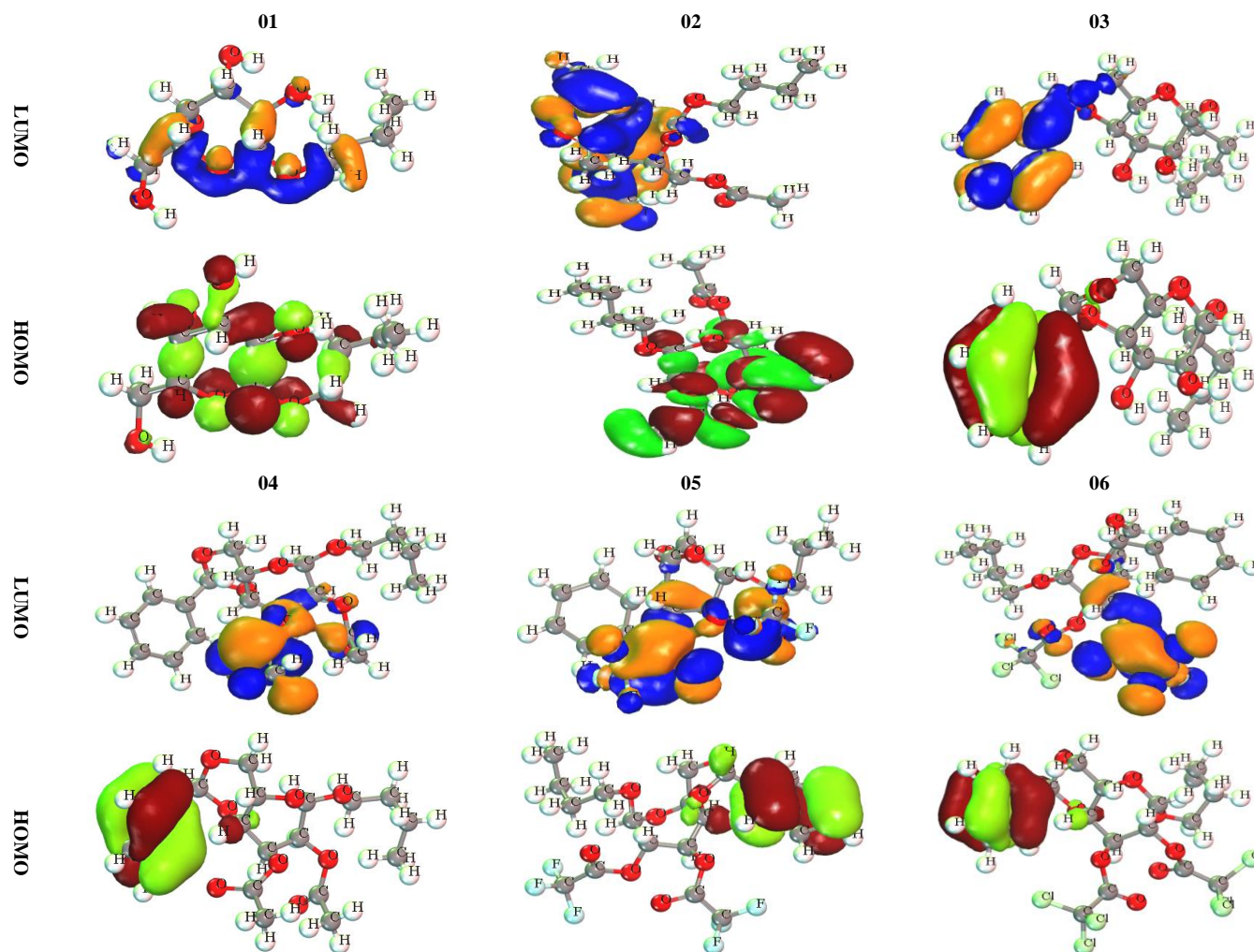


Figure 2. Frontier molecular orbitals diagram for HOMO and LUMO.

3.5 PASS prediction

All the designing compounds have provided the most potent Antineoplastic activity. The Pa value of all Ligands has been shown above 0.680+ and ligand N° 04 and 06 showed the highest Pa value (L04 Pa>0.884 & L06 Pa>0.931) while the smallest Pa value has been seen in L01 Pa>0.685. Even though the primary focus is on predicting Antineoplastic properties, additional prediction indicators

such as antiviral and antibacterial Pa values and antifungals have also been displayed in table 2.

The PASS prediction value is much higher against antineoplastic than antiviral, antibacterial, antibiotic & antifungal. It is almost opposed to the Pass prediction value of the traditional/standard drug. So, these higher values of Pa indicate that the bioactive molecules will act as a potential drug against breast cancer.

Table 2. Data of PASS prediction.

Ligand	Antiviral		Antibacterial		Antifungal		Antibiotic		Antineoplastic	
	Pa	Pi	Pa	Pi	Pa	Pi	Pa	Pi	Pa	Pi
01	0.345	0.024	0.531	0.014	0.675	0.011	0.314	0.013	0.685	0.029
02	0.264	0.052	0.561	0.011	0.774	0.009	0.334	0.011	0.838	0.008
03	0.335	0.026	0.362	0.040	0.661	0.012	0.202	0.028	0.817	0.010
04	0.296	0.038	0.383	0.034	0.633	0.015	0.199	0.029	0.884	0.005
05	0.226	0.076	0.190	0.127	0.486	0.033	0.179	0.024	0.773	0.015
06	0.217	0.082	0.256	0.080	0.601	0.018	0.134	0.057	0.931	0.005
07, Cyclophosphamide	0.235	0.111	N/A	N/A	N/A	N/A	N/A	N/A	0.996	0.003
08, Epirubicin hydrochloride	0.403	0.034	0.704	0.004	0.626	0.016	0.548	0.004	0.960	0.004

3.6 Molecular Docking

One of the most effective methods in structure-based drug design is docking that predicts the preferred orientation of a molecule and when bound to each other to form a stable complex and can indicate binding-conformity of small molecule ligands on suitable target sites. Since protein-ligand interaction plays a significant role in structurally based drug designing, H bonding and hydrophobic

bonding are the main reasons for docking scores. It is considered a standard drug if the docking score is above 6.00 kcal/mol (71). The main goal of molecular docking is to give a prediction of the ligand-receptor complex structure by using computation methods which can be obtained plays an significant role two interrelated steps: first by sampling Ligand's configurations on active sites of proteins; then arrange these distortions through a scoring function.

Table 3. Data of binding energy and name of interacted ligand for breast cancer protease (3hb5).

Ligand	Binding Affinity (kcal/mol)	No of H bond	No Hydrophobic bond	Halogen bond	Total bonds
01	-6.90	06	02	Absent	08
02	-8.10	04	05	Absent	09
03	-9.50	04	03	Absent	07
04	-8.60	03	02	Absent	05
05	-9.50	08	02	03	13
06	-8.80	02	02	Absent	04
07	-6.20	03	04	Absent	07
08	-10.40	07	04	Absent	11

MD and nonbonding interactions are performed to realize the binding affinity of all structures with the receptor protein. The present study is revealed that all drug molecules showed good binding energy toward the target protein ranging from -6.20 to -10.40 kcal/mol shown in table 3 and -5.70 to -7.90 kcal/mol in table 4. At the same time, 03, 05, and 08 could be considered the efficient inhibitor since the standard binding affinity has been considered -6.0 kcal/mol (72-78).

Table 4. Data of binding energy and name of interacted ligand for triple-negative breast cancer Protease (4pv5).

Ligand	Binding Affinity (kcal/mol)	No of H bond	No of Hydrophobic bond	No of van der Waal bond	Total bonds
01	-5.90	04	02	Absent	06
02	-6.20	02	02	Absent	04
03	-7.00	03	05	Absent	08
04	-7.40	01	08	Absent	09
05	-7.60	03	04	Absent	07
06	-7.40	02	02	Absent	04
07	-5.70	05	01	Absent	06
08	-7.90	03	04	Absent	07

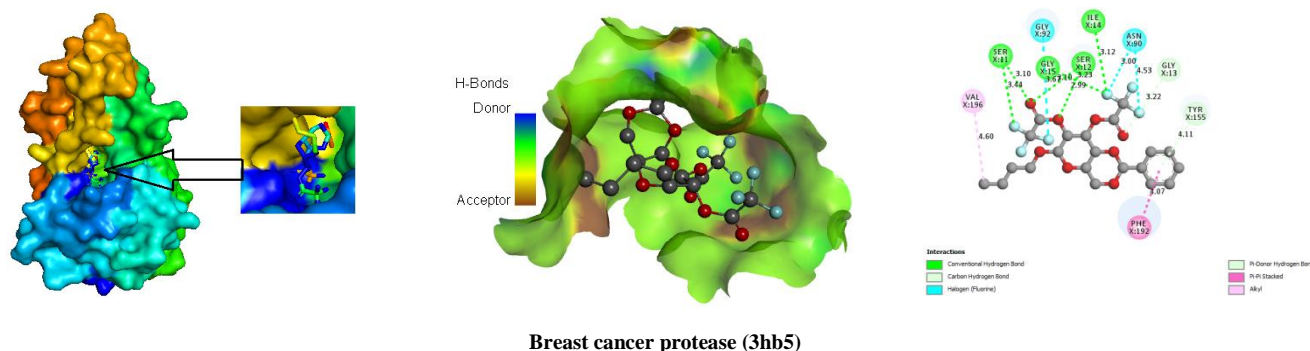
3.7 Protein-ligands interaction and binding sites

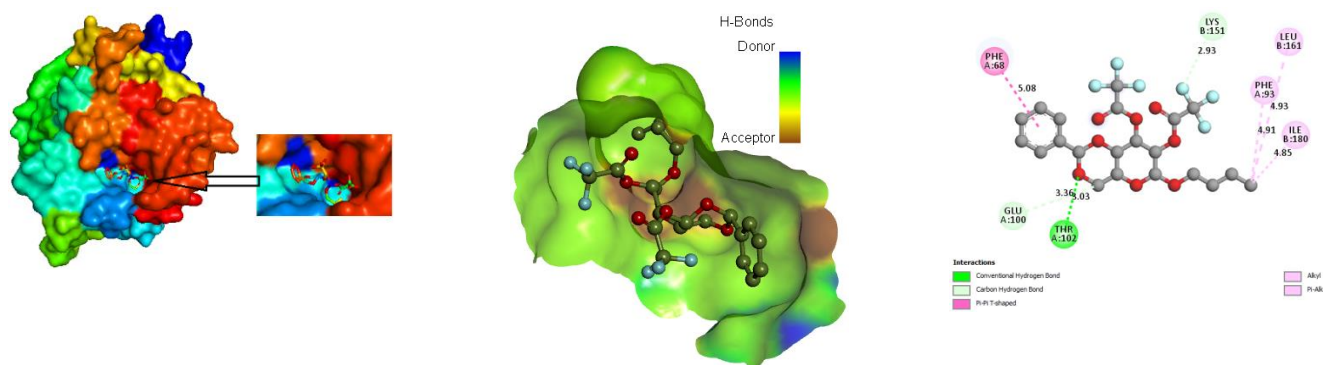
Protein-ligand interaction (PLI) has a significant role in discovering a new drug that provides vital information on the binding or bonding drugs with targeted pathogen proteins (79). However, it plays an essential role as a therapeutic goal. It is currently regarded as one of the most challenging areas of drug discovery due to specific structural characteristics of Protein interaction with ligands. The main protease of breast cancer protein, the interaction of drug molecules with 3hb5, has been investigated with bond distance. There are two types of bonds, H-bonds and hydrophobic bonds, but van der wall bonds are not presented for all drugs (table 4). The main protease and ligands interaction with amino acid residues and their bond distance is shown in Table 4.

The total active amino acid residues have been seen 22 before the docking study. These are THR-190, VAL-188, GLY-186, ILE-14, ALA-191, PHE-192, SER-12, ASN-90, LYS-159, SER-11, CYS-10, GLY-9, ALA-91, TYR-155, THR-135, LEU-36, ARG-37, VAL-66, ASP-65, ARG-67, LEU-64 and ARG-67.

Since the compounds 03, 05, and 08 have been obtained the highest binding affinities, it is observed that the Ligand 03 consists of a total of 07 active sides where four hydrogen PHE-192 (4.49), SER-12 (3.05), SER-12 (2.87), SER-12 (2.86) and PHE-192(3.39), PHE-192(4.82), ILE-4.38(4.38) residues are formed as a hydrophobic bond. On the other hand, compound no 05 consists of 10 active amino residues where 08 hydrogen bond SER-11 (3.10), SER-11(3.44), SER-12(3.67), SER-12(2.99), GLY-13(3.10). The GLY-13(3.22), ILE-14(3.12), TYR-155(4.11) are in the active sites, the VAL-196 (4.60), PHE-192 (4.07) are in hydrophobic bonds. Besides, compound no 08 has been obtained the 11 active amino acid portions, but the no of the hydrogen bond is higher number, such as PHE-192(5.73), PHE-192(4.80), SER-12(3.01), SER-12(3.25), SER-12(2.44), ALA-191(2.48), TYR-155 (2.88) compared to hydrophobic bond. These are performed against breast cancer Protease (3hb5).

Secondly, docking tests have been carried to combat triple-negative breast cancer protease (4pv5). First thing, before the docking tests, Triple-negative breast cancer Protease (4pv5) have consisted of fourteen (14) active sides; these included ASN-104, ARG-38, GLU-17, ARG-123, HIS-127, GLU-100, GLN-34, GLY-156, GLU-156, GLU-173, LYS-153, and GLU-100.





Triple-negative breast cancer protease (4pv5)

Figure 3. Various docking poses diagram for 05.

When the docking testing has been tested against triple-negative breast cancer Protease (4pv5), various active sites are obtained. The active sites have been observed GLU-173(3.45), GLU-173(2.08), GLU-100(2.35) hydrogen bond and ILE-180(4.46), LEU-61(5.07), PHE-63(4.98), PHE-163(4.70), LYS-151(5.40) for ligand 03. The Ligand 05 has been provided a total of 06 active sites, such as THR-102(3.03), GLU-100(3.36), LYS-151(2.93) as a hydrogen bond and PHE-68(5.08), LEU-161(4.93), PHE-93(4.91), ILE-180(4.85). In addition, ligand 08 has been supplied with a total of 07 active sites. Three hydrogen bonds PRO-167(2.64), GLN-165(2.03), GLN-165 (2.35), and four hydrophobic bonds PRO-167(4.49), PRO-167(4.44), LYS-148(5.03), LYS-148 (5.10), have been identified throughout them.

Table 5. Main protease and ligands interaction with amino acid residues and their bond distance (3hb5).

	Hydrogen bond		Hydrophobic bond		Halogen bond	
	Interacting residue of amino acid	Distance, Å	Interacting residue of amino acid	Distance, Å	Interacting residue of amino acid	Distance, Å
01	SER-12 SER-12 GLY-9 GLY-9 ASN-90 ILE-14	2.77 1.96 2.80 2.74 2.70 3.27	TYR-155 PHE-192	4.85 3.95	Absent	Absent
02	GLY-94 GLY-92 GLY-92 GLY-92 SER-12	2.94 3.13 3.22 3.19 2.83	ALA-191 PHE-192 PHE-192 TYR-155 ILE-14	4.30 3.68 5.05 4.91 4.50	Absent	Absent
03	PHE-192 SER-12 SER-12 SER-12	4.49 3.05 2.87 2.26	PHE-192 PHE-192 ILE-14	3.93 4.82 4.38	Absent	Absent
04	SER-11 SER-12 GLY-94	3.12 3.15 3.21	TYR-155 PHE-192	5.34 3.99	Absent	Absent
05	SER-11 SER-11 SER-12 SER-12 GLY-13 GLY-13 ILE-14 TYR-155	3.10 3.44 3.67 2.99 3.10 3.22 3.12 4.11	VAL-196 PHE-192	4.60 4.07	GLY-92 ASN-90 ASN-90	3.67 3.00 4.53
06	SER-12 GLY-94	2.90 3.01	TYR-155 PHE-192	4.94 3.97	Absent	Absent
07	GLY-92 LYS-159 TYR-155	3.42 3.55 2.55	PHE-192 PHE-192 VAL-196 MET-193	4.72 4.51 4.57 5.01	Absent	Absent
08	PHE-192 PHE-192 SER-12 SER-12 SER-12 ALA-191 TYR-155	5.73 4.80 3.01 3.25 2.44 2.48 2.88	PHE-192 PHE-192 PHE-192 MET-193	4.34 3.89 4.84 5.33	Absent	Absent

Table 6. Main protease and ligands interaction with amino acid residues and their bond distance.

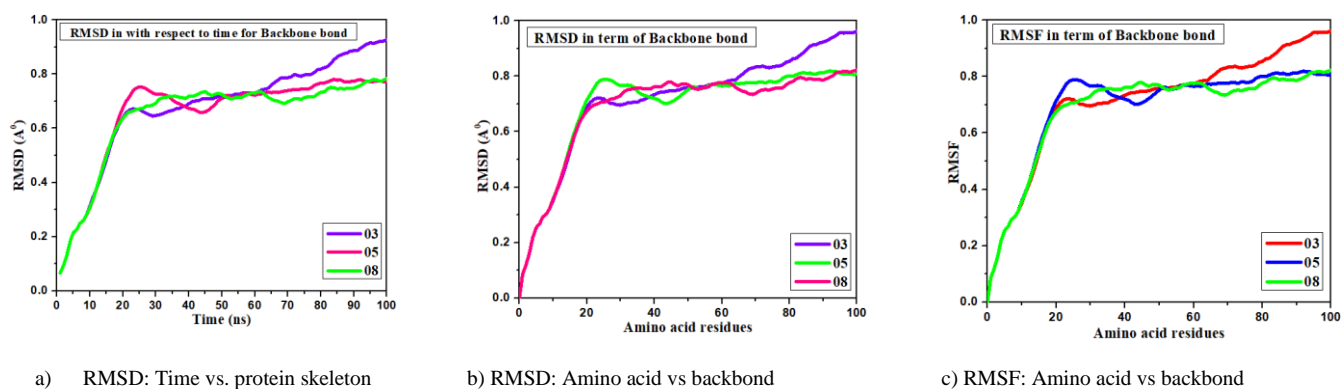
	Hydrogen bond		Hydrophobic bond		Halogen bond	
	Interacting residue of amino acid	Distance, Å	Interacting residue of amino acid	Distance, Å	Interacting residue of amino acid	Distance, Å
01	PHE-30 ASP-29 THR-56 THR-27	1.75 3.02 3.02 3.53	PRO-25 LYS-28	4.70 3.78	Absent	Absent
02	LYS-78 LYS-78	3.16 3.46	PHE-17 LEU-57	4.56 3.92		
03	GLU-173 GLU-173 GLU-100	3.45 2.08 2.35	ILE-180 LEU-61 PHE-63 PHE-163 LYS-151	4.46 5.07 4.98 4.70 5.40	Absent	Absent
04	THR-102	3.11	ILE-180 ILE-184 ILE-61 LEU-70 PHE-93 PHE-63 PHE-68 LYS-151	5.03 5.32 5.27 5.27 4.89 5.09 3.66 4.37		
05	THR-102 GLU-100 LYS-151	3.03 3.36 2.93	PHE-68 LEU-161 PHE-93 ILE-180	5.08 4.93 4.91 4.85	Absent	Absent
06	ASN-119 ARG-38	3.55 2.81	PHE-68 TRP-171	4.55 4.85		
07	TRP-105 HIS-103 SER-69 TYR-71 TYR-71	3.20 2.93 3.13 3.05 2.80	TRP-105	4.03	Absent	Absent
08	PRO-167 GLN-165 GLN-165	2.64 2.03 2.35	PRO-167 PRO-167 LYS-148 LYS-148	4.49 4.44 5.03 5.10	Absent	Absent

[Note: TRP = Tryptophan, ASP = Aspartic acid, GLU = Glutamic acid, LEU = Leucine, THR = Threonine, ASN = Asparagine, GLN = Glutamine, PHE = Phenylalanine, ILE = Isoleucine, ARG = Arginine, VAL = Valine, SER = Serine, PRO = Proline, GLY = Glycine, HIS = Histidine, LYS = Lysine, TRP = Tryptophan, CYS = Cysteine, MET = Methionine.]

3.8. Molecular Dynamics

Molecular dynamics (MD) is a widely applied computational method for analyzing the physical motion of atoms and molecules in each step of modern drug discovery (80). One of the notable methods of testing accuracy docking methods in case of average root-mean square deviation (RMSD) and root-mean square fluctuations (RMSF) is molecular mobility that provides accurate

information about the respective crystal structures' posture ligands and protein-interactions in complex structures. It has been revealed that the RMSD in the docking complex is less than 2 Å able to pose an excellent fitting ligand pose in the drug pocket and compactly dock the software. Then create both docked poses in parallel with the docked complex by RMSD; Low values indicate the accuracy and durability of the docking method.

**Figure 4.** Various pictures of RMSD and RMSF for Breast cancer Protease (3hb5).

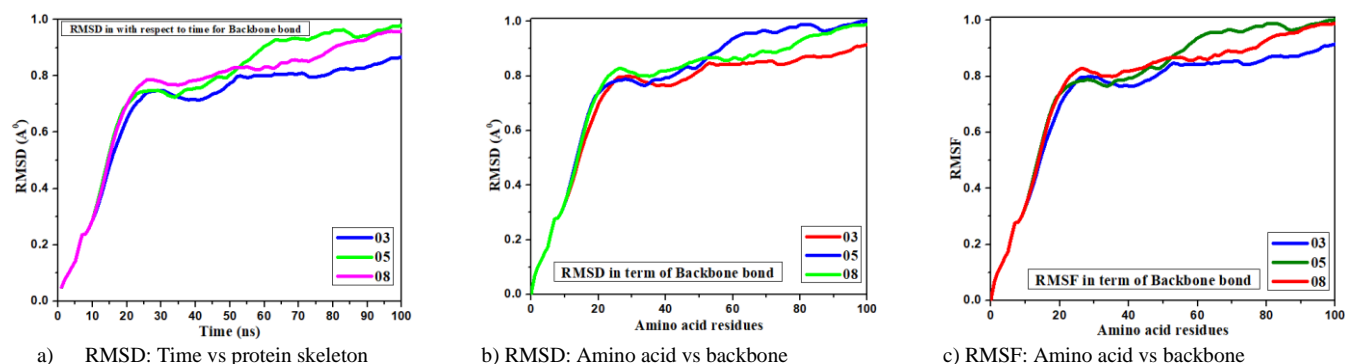


Figure 5. Various pictures of RMSD and RMSF for Triple-negative breast cancer Protease (4pv5).

3.9. Pharmacokinetics and Drug likeness study

The concept of pharmacokinetics and drug-likeness provides valuable guidance in the earliest phases of drug development to improve the chances of a chemical entry and clinical passage—SwissAdME forecasting of Pharmacokinetics and characteristics of drug molecules. The nonfigurative drug discovery of molecular information on the pharmacokinetics features of the molecule must be achieved at an early stage (81). Pharmacokinetics and drug-similarity have been studied comparatively as Lipinski's rule of thumb and drug

activity, using the online database link <https://www.sib.swiss/>, provided by the Swiss Institute of Bioinformatics to develop a new drug for breast cancer. From table 6, it is clear that all selected molecules follow the Lipinski rule as drugs. All the drugs have a high absorption rate in the GI, which means the drug has been absorbed very rapidly in the GI absorption of all drugs excluded ligand 08. Besides, the bioavailability of all drug are reported much better than that refers while the drug will be taken orally, the extent rate of the active moiety (drug or metabolite) enters and is present in systemic circulation very rapidly.

Table 7. Data of Lipinski rule, Pharmacokinetics, and Druglikeness.

	NBR	HBA	HBD	TPSA, Å ²	Consensus Log Po/w	Log Kp (skin permeation), cm/s	Lipinski rule		MW	Bioavailability Score	GI absorption
							Result	violation			
01	5	6	4	99.38	-0.60	-8.48	Yes	0	236.26	0.55	High
02	11	8	0	97.36	1.86	-7.23	Yes	0	360.40	0.55	High
03	5	6	2	77.38	1.37	-7.48	Yes	0	324.37	0.55	High
04	9	8	0	89.52	2.34	-7.18	Yes	0	408.44	0.55	High
05	11	14	0	89.52	3.95	-6.25	Yes	1	516.38	0.55	High
06	11	8	0	89.52	4.56	-5.81	Yes	1	615.11	0.55	High
07	5	4	1	51.38	1.23	-7.45	Yes	0	261.09	0.55	High
08	5	12	6	206.07	0.50	-8.71	No	3	543.52	0.17	Low

3.10 Pharmacokinetics and ADMET studies

An essential part of developing drugs is the DMPK investigations. These have sometimes been alluded to as ADMET (Absorption, Distribution, Metabolism, Elimination, and Toxicity) analyses since they investigate how drugs are metabolized and how they are eliminated from the body (82). These investigations assist in determining a medication candidate's effectiveness (83). Firstly, the Absorption – exactly how much and how promptly is the medication is absorbed (84), Distribution- after administration of any therapeutic drug, where the medication is dispersed inside the body and how quickly and widely it has been delivered (85). Metabolism - how quickly does the medication break down, the mode of action, the metabolite form generated, and whether it is

effective or poisonous (86), elimination- this has been described that in what way and how promptly does the medication leaves the body (87) and toxicity- this has been described. Is this medication harmful to the organ functions or provided any detrimental effect (88).

The ADMET nature of the drug obtained from an online database for computational forecasting, as shown in Table 7. All the therapeutic candidates are rapidly absorbed in human intestinal absorption which is illustrated around 0.7928 to 0.9695. They can easily cross the blood-brain barrier, and all the sub-cellular localization therapeutic compounds have been seen in Mitochondria. And they cannot inhibit of CYP450 1A2 Inhibitor which means drug cannot accumulation to the body and no chance to the P- I glycoprotein inhibitor and P- II glycoprotein substrate.

Table 8. Pharmacokinetics and ADMET Data.

SL	Human Intestinal Absorption	Caco-2 Permeability	Blood-Brain Barrier	P- I glycoprotein inhibitor	P- II glycoprotein substrate	Renal Organic Cation Transporter	Sub-cellular localization	CYP450 2C9 Substrate	CYP450 1A2 Inhibitor
01	0.9695	-0.8230	Yes	No	No	No	Mitochondria	No	No
02	0.7508	0.7423	Yes	No	No	No	Mitochondria	No	No
03	0.8983	-0.6167	Yes	No	Yes	No	Mitochondria	No	No
04	0.7928	0.5763	Yes	Yes	Yes	No	Mitochondria	No	No
05	0.8300	0.6352	Yes	Yes	Yes	No	Mitochondria	No	No
06	0.8090	-0.7474	Yes	Yes	Yes	No	Mitochondria	No	No
07	0.8675	0.6137	Yes	No	No	No	Mitochondria	No	No
08	0.8447	-0.8650	Yes	No	Yes	No	Mitochondria	No	No

3.11. Toxicity

Toxicity describes how much harmful effect a drug-like substance may have on a living organism (88). Toxicity data has been recorded for all medications listed in table 8 for aquatic and non-aquatic environments. It was found that all the drugs are strongly soluble in the water medium and the range of aqua solubility -0.406 to -5.12 where the highest solubility is -5.12 for 05 and the lowest values is 0.406 for 01. Besides, all the compounds have no adverse effect

on the environment, non-toxic, non-carcinogenic, and are readily absorbed by the human body. There was a wide variation in the acute oral toxicity of the industrial chemicals, with a value range of 1.3384 kg/mol to 2.7694 kg/mol. Since all the ligands have been free from carcinogenicity, it can be said that there is no chance to create cancer in the living organism. On the other hand, it has been found that the reported ligands are also non-toxic, which has been referred that the ligands have no possibility to produce any harmful effect on both environment and human health.

Table 9. Aquatic and non-aquatic toxicity.

S. L	AMES toxicity	Carcinogenicity	Water solubility, Log S	Plasma protein binding	Acute Oral Toxicity, kg/mol	Oral Rat Acute Toxicity (LD50) (mol/kg)	Fish Toxicity pIC ₅₀ mg/L	T. Pyriiformis toxicity (log ug/L)
01	No	No	-0.406	0.406	3.297	1.3384	2.5014	-0.4367
02	No	No	-2.216	0.62	2.106	1.7873	1.0241	0.3164
03	No	No	-3.647	0.89	2.743	2.3579	1.1753	0.8258
04	No	No	-4.714	0.706	2.543	2.2923	0.2275	1.068
05	No	No	-4.806	1.025	2.37	2.7694	0.0986	1.3551
06	No	No	-5.12	1.016	3.127	2.6702	0.0284	1.4345
07	No	No	-2.605	0.255	3.421	3.3855	2.1973	0.0985
08	No	No	-2.719	0.924	3.219	2.6644	1.3320	0.3955

3.12 QSAR and pIC₅₀

One of the most commonly utilized techniques in ligand-based drug design is the quantitative structure-activity relationship (QSAR) (89). Using computational techniques, the QSAR calculation was done to identify the correlation between the biological and structural activities of bioactive

molecules. The overall value of the QSAR and pIC₅₀ assessment satisfies all requirements, and substances have varied QSAR as well as pIC₅₀ in different compounds. The QSAR and pIC₅₀ ranges are discovered to be between 4.3321 and 5.1462, with 5.1462 being the highest and 4.3321 being the lowest. The calculated pIC₅₀ (Table 8) implies that these described compounds may be therapeutically effective against breast cancer.

QSAR data here, pIC₅₀

$$\text{(Activity)} = -2.768483965 + 0.133928895 \times (\text{Chiv5}) + 1.59986423 \times (\text{bcutm1}) + (-0.02309681) \times (\text{MRVSA9}) + (-0.002946101) \times (\text{MRVSA6}) + (0.00671218) \times (\text{PEOEVSAS}) + (-0.15963415) \times (\text{GATSv4}) + (0.207949857) \times (\text{J}) + (0.082568569) \times (\text{Diameter}).$$

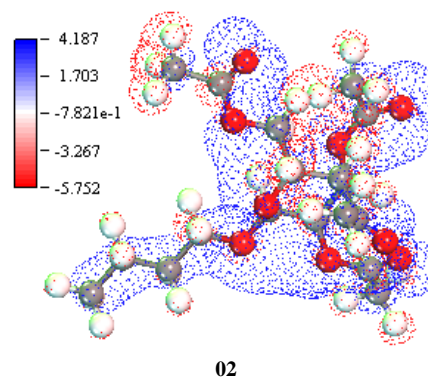
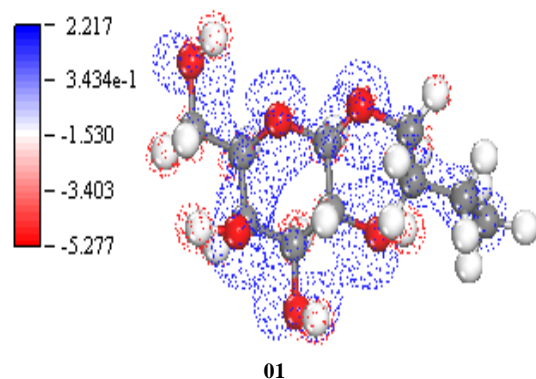
Table 10. QSAR and pIC₅₀

	Chiv5	bcutm1	MRVSA9	MRVSA6	PEOEVSAS	GATSv4	J	Diameter	pIC ₅₀
01	0.971	3.74	0.000	0.000	13.345	1.053	2.496	09.000	4.5287
02	1.852	3.79	17.908	0.000	20.268	1.188	2.926	11.000	4.5925
03	2.022	3.859	0.000	35.895	43.676	1.240	1.561	14.000	5.1462
04	2.539	3.87	11.939	35.895	43.676	1.259	1.753	14.000	4.9942
05	2.565	3.874	11.939	35.895	43.676	1.050	1.880	14.000	5.0639
06	2.874	4.126	81.544	35.895	113.282	1.275	1.880	14.000	4.3321
07	2.869	4.414	30.872	0.000	0.000	1.059	2.531	07.000	4.8998
08	4.116	4.078	17.350	51.58	12.133	1.104	1.485	14.000	5.1243

3.13. 3D Potential Map of electrostatic potential charge distribution

The electrostatic potential is used to conjecture chemical reactivity since parts of negative potential charge represent the protonation and nucleophilic attack areas, whereas sections of positive potential charge may imply electrophilic sites. Electrostatic potentials have been extensively employed in investigating many

biological, physical, and practices and analyses (90-92). The positive electrostatic potential area has been colored in blue (electrophilic site), and the red color area indicated the nucleophilic binding sites below figure 7. It has been seen that the blue color (electrophilic site) is more prominent compared to nucleophilic binding sites.



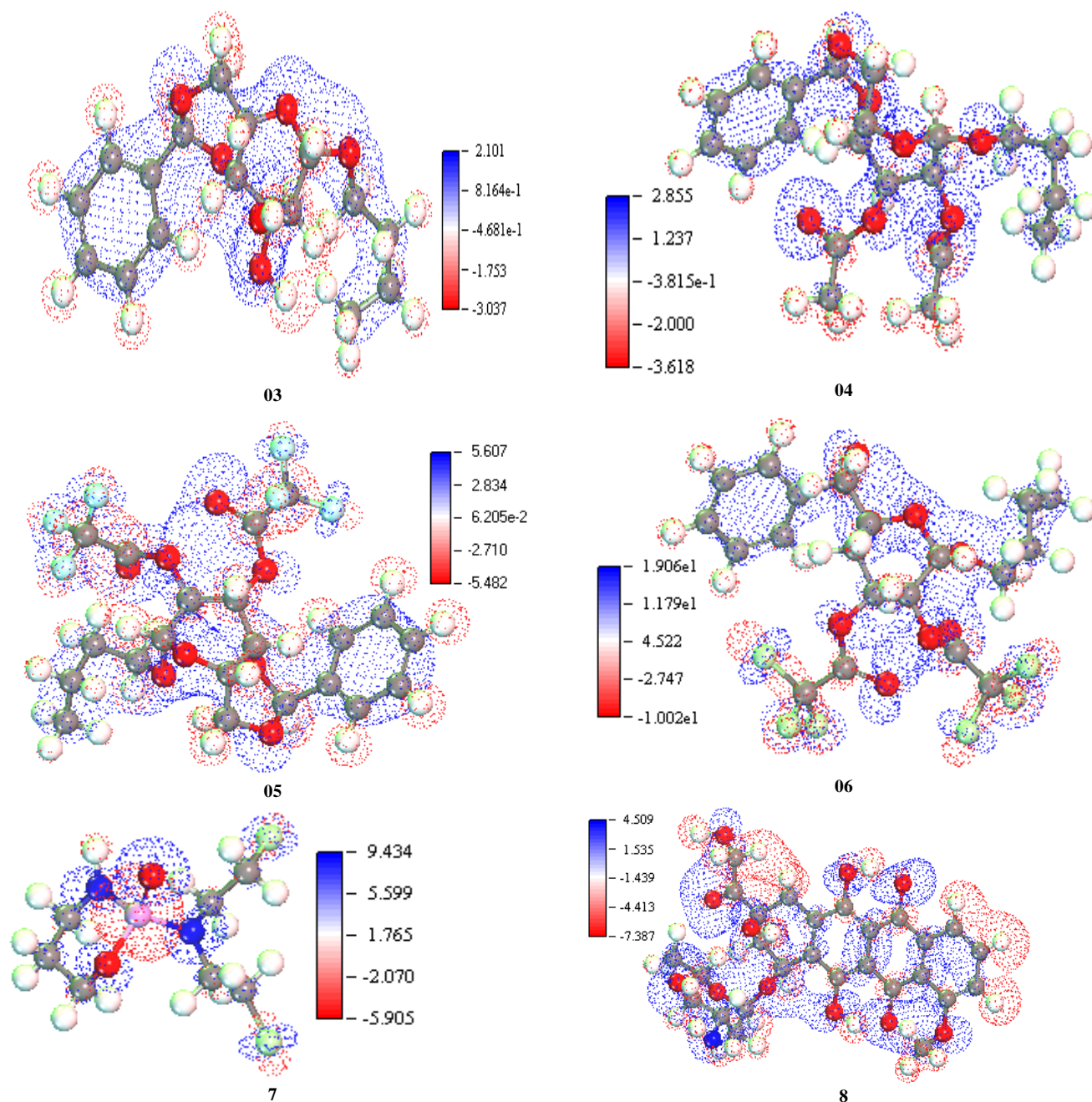


Figure 6. 3D Potential Map of electrostatic potential charge distribution.

CONCLUSION

In this study, the computationally design and tools have been carried out applying D-glucufuranose, as well as its modifications form (derivatives) against breast cancer Protease (3hb5) and triple-negative breast cancer protease (4pv5), with computational models employing computer simulations being used to generate innovative synthesized active compounds. The molecular docking has been used to calculate the binding affinity against breast cancer protease (3hb5) and triple-negative breast cancer protease (4pv5) to acquire a more realistic investigation. The maximum docking score has documented in such a range is at -9.5 kcal/mol against breast cancer for 03 and 05. Secondly, it conveys at -8.80 and -8.60 kcal/mol for 06 and 04, respectively, which magnitude is much more significant for being an effective drug. However, compared to standard substances, it is possible to extrapolate that the assessed ligand has almost a similar binding affinity and an equivalent illustration for RMSD and RMSF molecular dynamic accountancy to show its stability. After the overall analysis, it has been seen that the entire drug candidates are highly soluble in water, free from carcinogens with high GI absorption, accomplished the Lipinski rule and

attributes of drug-likeness features. So, it has been decided that the finding of new potential drug candidates 03, 05, and 08 could be considered the standard drug. Since these drugs have fulfilled all the parameters, hopefully, if they are brought to the commercial market, they are much safer than preexisting drugs. The side effects will also be less than Preexisting medication, which has already been available in the market like chemotherapy.

CONFLICTS OF INTEREST

There are no conflicts to declare.

AUTHOR CONTRIBUTIONS

AK designed, optimized and docking of molecules wrote the manuscript; UC performed the molecular dynamic and analysis the obtained data; DH, SA, and MEK were equally contributed to take the obtained data, and took 2D and 3D picture, protein–ligand interaction; and TH gave all technical supports. MMM reviewed the full paper. Finally, all authors gave final approval for publication.

ACKNOWLEDGMENT

We are thankful to Laboratory of Computational Research for Drug Design and Material Science, Department of Chemistry, European University of Bangladesh, Gabtoli, Dhaka-1216, Bangladesh for their all computational supports, and University of Chittagong for their working supports.

FUNDING NOTE

No Funding was obtained from my university even any institutions.

REFERENCES

- Lehmann, J., DeLisa, J., Warren, C., Bryant, P., and Nicholson, C. (1978) Cancer rehabilitation: assessment of need, development, and evaluation of a model of care, *Archives of physical medicine and rehabilitation* 59, 410-419.
- Wang, H., Naghavi, M., Allen, C., Barber, R. M., Bhutta, Z. A., Carter, A., Casey, D. C., Charlson, F. J., Chen, A. Z., and Coates, M. M. (2016) Global, regional, and national life expectancy, all-cause mortality, and cause-specific mortality for 249 causes of death, 1980–2015: a systematic analysis for the Global Burden of Disease Study 2015, *The lancet* 388, 1459-1544.
- Nagai, H., and Kim, Y. H. (2017) Cancer prevention from the perspective of global cancer burden patterns, *Journal of thoracic disease* 9, 448.
- Sharma, G. N., Dave, R., Sanadya, J., Sharma, P., and Sharma, K. (2010) Various types and management of breast cancer: an overview, *Journal of advanced pharmaceutical technology & research* 1, 109.
- Parsa, N. (2012) Environmental factors inducing human cancers, *Iranian journal of public health* 41, 1.
- Diet and Physical Activity: What's the Cancer Connection? (<https://www.cancer.org/cancer/cancer-causes/diet-physical-activity/diet-and-physical-activity.html>), *American cancer society*.
- Fromer, M. (2007) New SEER report documents high risk of second cancers in cancer survivors, *Oncology Times* 29, 8.
- Ershler, W. B. (2005) The influence of advanced age on cancer occurrence and growth, *Biological Basis of Geriatric Oncology*, 75-87.
- Stage, I., and Stage, I. Breast cancer happens when cells in your breast grow and divide in an uncontrolled way, creating a mass of tissue called a tumor. The risk of developing breast cancer increases you age and with weight gain. Signs of breast cancer can include feeling a lump in a breast, experiencing a change in the size of your breast and seeing changes to the skin on your breasts. Early detection is aided by mammograms.
- Khuwaja, G. A., and Abu-Rezq, A. (2004) Bimodal breast cancer classification system, *Pattern analysis and applications* 7, 235-242.
- Buja, A., Pierbon, M., Lago, L., Grotto, G., and Baldo, V. (2020) Breast cancer primary prevention and diet: An umbrella review, *International journal of environmental research and public health* 17, 4731.
- Martin, A.-M., and Weber, B. L. (2000) Genetic and hormonal risk factors in breast cancer, *Journal of the National Cancer Institute* 92, 1126-1135.
- Tyrer, J., Duffy, S. W., and Cuzick, J. (2004) A breast cancer prediction model incorporating familial and personal risk factors, *Statistics in medicine* 23, 1111-1130.
- Thomas, D. B. (1984) Do hormones cause breast cancer?, *Cancer* 53, 595-604.
- Singh, P., Kapil, U., Shukla, N., Deo, S., and Dwivedi, S. (2011) Association of overweight and obesity with breast cancer in India, *Indian journal of community medicine: official publication of Indian Association of Preventive & Social Medicine* 36, 259.
- Arce-Salinas, C., Aguilar-Ponce, J., Villarreal-Garza, C., Lara-Medina, F., Olvera-Caraza, D., Miranda, A. A., Flores-Diaz, D., and Mohar, A. (2014) Overweight and obesity as poor prognostic factors in locally advanced breast cancer patients, *Breast cancer research and treatment* 146, 183-188.
- Lynch, B. M., Neilson, H. K., and Friedenreich, C. M. (2010) Physical activity and breast cancer prevention, *Physical activity and cancer*, 13-42.
- Monninkhof, E. M., Elias, S. G., Vleems, F. A., van der Tweel, I., Schuit, A. J., Voskuil, D. W., and van Leeuwen, F. E. (2007) Physical activity and breast cancer: a systematic review, *Epidemiology*, 137-157.
- (2018.) Breast cancer statistics (<https://www.wcrf.org/dietandcancer/breast-cancer-statistics/>).
- Mazumdar, M., Fournier, D., Zhu, D.-W., Cadot, C., Poirier, D., and Lin, S.-X. (2009) Binary and ternary crystal structure analyses of a novel inhibitor with 17 β -HSD type 1: a lead compound for breast cancer therapy, *Biochemical Journal* 424, 357-366.
- Zhang, H., Huang, Q., Zhai, J., Zhao, Y.-n., Zhang, L.-p., Chen, Y.-y., Zhang, R.-w., Li, Q., and Hu, X.-p. (2015) Structural basis for 18- β -glycyrrhetic acid as a novel non-GSH analog glyoxalase I inhibitor, *Acta Pharmacologica Sinica* 36, 1145-1150.
- Myers, S. B., Ann. (2001) Drug discovery—an operating model for a new era, *Nature biotechnology* 19, 727-730.
- DiMasi, J. A. H., Ronald W; Grabowski, Henry G. (2003) The price of innovation: new estimates of drug development costs, *Journal of health economics* 22, 151-185.
- Nicolaou, K. (2014) Advancing the drug discovery and development process, *Angewandte Chemie* 126, 9280-9292.
- Zhao, H., Zong, G., Zhang, J., Wang, D., and Liang, X. (2011) Synthesis and anti-fungal activity of seven oleanolic acid glycosides, *Molecules* 16, 1113-1128.
- Matin, M. M. B., MMH; Debnath, Dulal C; Manchur, MA. (2013) Synthesis and comparative antimicrobial studies of some acylated D-glucopyranose and D-glucopyranose derivatives, *Int. J. Biosci* 3, 279-287.
- Nizamov, I. S. N., Yevgeniy N; Nizamov, Inar D; Belov, Timur G; Voloshina, Alexandra D; Batyeva, Elvira S; Cherkasov, Rafael A. (2016) α -D-Glucopyranose and α -D-allofuranose diacetone and silyl ether of α -D-glucopyranose diacetone in dithiophosphorylation reactions, *Heteroatom Chemistry* 27, 345-352.
- Benedeković, G. P., Mirjana; Radulović, Niko S; Stojanović-Radić, Zorica; Farkas, Sándor; Francuz, Jovana; Popsavin, Velimir. (2021) Synthesis and antimicrobial activity of (-)-cleistenolide and analogues, *Bioorganic Chemistry* 106, 104491.
- Matin, M. M. B., Md Mosharef Hossain; Azad, Abul Kalam Mohammad Shamsuddin; Rashid, Md Harun Or. (2015) Synthesis of 6-O-Stearoyl-1, 2-O-isopropylidene-[alpha]-D-glucopyranose derivatives for antimicrobial evaluation, *Journal of Physical Science* 26, 1.
- Ouchi, T., Jokei, S., Fujie, H., Chikashita, H., and Inoi, T. (1984) Synthesis of 1, 2: 5, 6-Di-O-isopropylidene-3-O-[3-(5-fluorouracil-1-yl)-propionyl]- α -D-glucopyranose and its antitumor activity, *Journal of heterocyclic chemistry* 21, 1023-1024.
- Kawsar, S. M. A. I., Md Moinul; Chowdhury, Shagir Ahammad; Hasan, Tanvirul; Hossain, Mohammed Kamrul; Manchur, Mohammad Abul, and Ozeki, Y. (2013) Design and newly synthesis of some 1, 2-O-isopropylidene- α -D-glucopyranose derivatives: Characterization and antibacterial screening studies, *Hacettepe Journal of Biology and Chemistry* 41, 195-206.
- REIST, E. J., SPENCER, R. R., WAIN, M. E., JUNGA, I. G., GOODMAN, L., and Baker, B. (1961) Potential Anticancer Agents. 1 LVII. Synthesis of Alkylating Agents Derived from 6-Amino-6-deoxy-D-glucose and 5-Amino-5-deoxy-D-ribose, *The Journal of Organic Chemistry* 26, 2821-2827.
- Ramos, J. (2020) Introducción a Materials Studio en la Investigación Química y Científica de los Materiales.
- Delley, B. (1995) DMol, a standard tool for density functional calculations: review and advances, In *Theoretical and computational chemistry*, pp 221-254; [https://doi.org/210.1016/S1380-7323\(1005\)80037-80038](https://doi.org/210.1016/S1380-7323(1005)80037-80038), Elsevier.
- Delley, B. (2010) Time dependent density functional theory with DMol3, *Journal of Physics: Condensed Matter* 22, 384208.
- Kadir, F. A., Kassim, N. M., Abdulla, M. A., and Yehye, W. A. (2013) PASS-predicted Vitex negundo activity: antioxidant and antiproliferative properties on human hepatoma cells-an in vitro study, *BMC complementary and alternative medicine* 13, 1-13.
- DeLano, W. L. (2002) The PyMOL user's manual, <http://www.pymol.org>.
- Dallakyan, S., and Olson, A. J. (2015) Small-molecule library screening by docking with PyRx, In *Chemical biology*, pp 243-250, Springer.
- Inc, A. S. (2017) Discovery Studio Modeling Environment, Release 4.0, Accelrys Software Inc San Diego.
- James C. Phillips, D. J. H., Julio D. C. Maia, John E. Stone, Joao V. Ribeiro, Rafael C. Bernardi, Ronak Buch, Giacomo Fiorin, Jerome Henin, Wei Jiang, Ryan McGreevy, Marcelo C. R. Melo, Brian K. Radak, Robert D. Skeel, Abhishek Singharoy, Yi Wang, Benoit Roux, Aleksei Aksimentiev, Zaida Luthey-Schulten, Laxmikant V. Kale, Klaus Schulten, Christophe Chipot, and Emad Tajkhorshid. (2020) Scalable molecular dynamics on CPU and GPU architectures with NAMD, *Journal of Chemical Physics*, 153, 044130; <https://doi.org/044110.041063/044135.0014475>.
- Skjevik, Å. A., Madej, B. D., Dickson, C. J., Teigen, K., Walker, R. C., and Gould, I. R. (2015) All-atom lipid bilayer self-assembly with the AMBER and CHARMM lipid force fields, *Chemical Communications* 51, 4402-4405.
- Lipinski, C. A. J. d. t. T. (2004) Lead-and drug-like compounds: the rule-of-five revolution, *1*, 337-341.

43. Walters, W. P., Murcko, A. A., and Murcko, M. A. J. C. o. i. c. b. (1999) Recognizing molecules with drug-like properties, *3*, 384-387.
44. Walters, W. P., and Murcko, M. A. J. A. d. d. r. (2002) Prediction of 'drug-likeness', *54*, 255-271.
45. Daina, A., Michielin, O., and Zoete, V. J. S. r. (2017) SwissADME: a free web tool to evaluate pharmacokinetics, drug-likeness and medicinal chemistry friendliness of small molecules, *7*, 1-13.
46. Daina, A., Michielin, O., and Zoete, V. (2017) SwissADME: a free web tool to evaluate pharmacokinetics, drug-likeness and medicinal chemistry friendliness of small molecules, *Scientific reports* *7*, 1-13.
47. Cheng, F. L., Weihua; Zhou, Yadi; Shen, Jie; Wu, Zengrui; Liu, Guixia; Lee, Philip W; Tang, Yun;. (2012) admetSAR: a comprehensive source and free tool for assessment of chemical ADMET properties, *J Chem Inf Model* *52*, 3099-3105. doi: 3010.1021/ci300367a.
48. Hongbin Yang, C. L., Lixia Sun, Jie Li, Yingchun Cai, Zhuang Wang, Weihua Li, Guixia Liu, Yun Tang;. (2018) admetSAR 2.0: web-service for prediction and optimization of chemical ADMET properties, *Bioinformatics* *35*, 1067-1069. <https://doi.org/10.1093/bioinformatics/bty1707>.
49. Yang, H. L., Chaofeng; Sun, Lixia; Li, Jie; Cai, Yingchun; Wang, Zhuang; Li, Weihua; Liu, Guixia; Tang, Yun;. (2019) admetSAR 2.0: web-service for prediction and optimization of chemical ADMET properties, *Bioinformatics* *35*, 1067-1069.
50. Dewar, M. J., Zebisch, E. G., Healy, E. F., and Stewart, J. J. J. o. t. A. C. S. (1985) Development and use of quantum mechanical molecular models. 76. AM1: a new general purpose quantum mechanical molecular model, *107*, 3902-3909.
51. De Oliveira, D. B. G., Anderson Coser. (2000) BuildQSAR: a new computer program for QSAR analysis, *Quantitative Structure-Activity Relationships: An International Journal Devoted to Fundamental and Practical Aspects of Electroanalysis* *19*, 599-601.
52. Wang, S., Dong, G., and Sheng, C. (2019) Structural simplification: an efficient strategy in lead optimization, *Acta Pharmaceutica Sinica B* *9*, 880-901.
53. Ahmed, T. (2015) Design and Development of Drugs Targeting Molecular Structures of Genes and Proteins, East West University.
54. Lu, L. (2015) Can B3LYP be improved by optimization of the proportions of exchange and correlation functionals?, *International Journal of Quantum Chemistry* *115*, 502-509.
55. Aihara, J.-i. (1999) Reduced HOMO– LUMO gap as an index of kinetic stability for polycyclic aromatic hydrocarbons, *The Journal of Physical Chemistry A* *103*, 7487-7495.
56. Afroza, Z. K., Ajoy; Sarker, Md. Nuruzzaman; Paul, Sunanda. (2019) The substituent group activity in the anion of cholinium carboxylate ionic liquids on thermo-physical, chemical reactivity, and biological properties: A DFT study, *International Journal of Chemistry and Technology* *3*, 151-161; 110.32571/ijct.648409.
57. Ajoy, K., ; Sunanda, Paul; Md., Nuruzzaman, Sarker; Mohammad, Jahidul, Islam;. (2019) The prediction of thermo physical, vibrational spectroscopy, chemical reactivity, biological properties of morpholinium borate, phosphate, chloride and bromide Ionic Liquid: A DFT Study, *International Journal of New Chemistry* *6*, 236-253. <https://dx.doi.org/210.22034/ijnc.22019.110412.111053>.
58. Ajoy, K., ; Islam, Mohammad Jahidul; Paul, Sunanda;. (2020) Effect of External Electric Field and Temperature on Entropy, Heat of Capacity, and Chemical Reactivity with QSAR Study of Morphonium Chloride and Nitrous Ionic Liquids Crystal Using DFT, *Chemical Methodologies* *4*, 595-604.
59. Kumer, A., ; Sarker, Md., Nuruzzaman; Paul, Sunanda; Zannat, Afroza;. (2019) The Theoretical Prediction of Thermophysical properties, HOMO, LUMO, QSAR and Biological Indics of Cannabinoids (CBD) and Tetrahydrocannabinol (THC) by Computational Chemistry, *Advanced Journal of Chemistry-Section A* *2*, 190-202; doi-110.33945/SAMI/AJCA.32019.33942.190202.
60. Kumer, A., ; Sarker, Md Nuruzzaman; Paul, Sunanda;. (2019) The theoretical investigation of HOMO, LUMO, thermophysical properties and QSAR study of some aromatic carboxylic acids using HyperChem programming, *International Journal of Chemistry and Technology* *3*, 26-37.
61. Kumer, A., ; Sarker, Md Nuruzzaman; Paul, Sunanda;. (2019) The thermo physical, HOMO, LUMO, Vibrational spectroscopy and QSAR study of morphonium formate and acetate Ionic Liquid Salts using computational method, *Turkish Computational and Theoretical Chemistry* *3*, 59-68; <https://dergipark.org.tr/tr/download/article-file/723558>.
62. Kumer, A., ; Sarker, Md., Nuruzzaman; Pual, Sunanda;. (2019) The Simulating Study of HOMO, LUMO, thermo Physical and Quantitative Structure of Activity Relationship (QSAR) of Some Anticancer Active Ionic Liquids, *Eurasian Journal of Environmental Research* *3*, 1-10; <https://dergipark.org.tr/en/pub/ejere/issue/45416/478362>.
63. Sunanda Paul; Ajoy Kumer; Md Nuruzzaman, S., ; Islam, Mohammad Jahidul;. (2020) The effect of halogen atoms at propanoate anion on thermo physical, vibrational spectroscopy, chemical reactivity, biological properties of morpholinium propionate Ionic Liquid, *International journal of Advanced Biological and Biomedical Research* *8*, 112-127.
64. Islam, M., Jahidul; Kumer, Ajoy; Sarker, Md., Nuruzzaman; Paul, Sunanda; Zannat, Afroza. (2019) The prediction and theoretical study for chemical reactivity, thermophysical and biological activity of morpholinium nitrate and nitrite ionic liquid crystals: A DFT study, *Advanced Journal of Chemistry-Section A* *2*, 316-326. <http://dx.doi.org/310.33945/SAMI/AJCA.32019.33944.33945>.
65. Islam, M. J., ; Sarker, Md. Nuruzzaman; Kumer, Ajoy; Paul, Sunanda;. (2019) The Evaluation and Comparison of Thermo-Physical, Chemical and Biological Properties of Palladium(II) Complexes on Binuclear Amine Ligands with Different Anions by DFT Study, *International journal of Advanced Biological and Biomedical Research* *7*, 318-337. <https://dx.doi.org/310.33945/SAMI/IJABBR.32019.33944.33943>.
66. Islam, M. J., ; Kumer, Ajoy; Paul, Sunanda; Sarker, Md Nuruzaman;. (2020) The Activity of Alkyl Groups in Morpholinium Cation on Chemical Reactivity, and Biological Properties of Morpholinium Tetrafluoroborate Ionic Liquid Using the DFT Method, *Chemical Methodologies* *4*, 130-142. <http://dx.doi.org/110.33945/SAMI/CHEMM.32020.33942.33943>.
67. Kumer, A. I., Mohammad Jahidul; Paul, Sunanda;. (2020) Effect of External Electric Field and Temperature on Entropy, Heat of Capacity, and Chemical Reactivity with QSAR Study of Morphonium Chloride and Nitrous Ionic Liquids Crystal Using DFT, *Chemical Methodologies* *4*, 595-604.
68. Md, N. S. A., Kumer; Mohammad, Jahidul Islam; Sunanda, Paul;. (2019) A computational study of thermophysical, HOMO, LUMO, vibrational spectrum and UV-visible spectrum of cannabicyclol (CBL), and cannabigerol (CBG) using DFT, *Asian Journal of Nanoscience and Materials* *2*, 439-447.
69. Mohammad, J., Islam; Sunanda, Paul; Ajoy, Kumer; Md., Nuruzzaman, Sarker. (2020) Computational approach of palladium (II) complex ions with binuclear diamine ligands thermo-physical, chemical, and biological properties: a dft study, *Asian Journal of Nanosciences and Materials* *3*, 67 -81.
70. Mohammad, J., Islam, Md, N., Sarker, Ajoy, K., and Sunanda, P. (2019) The Comparison of Primary, Secondary and Tertiary Amine Ligands on Palladium (II) Complex Ion on Thermo-Physical, Chemical Reactivity, and Biological Properties: A DFT Study, *Cumhuriyet Science Journal* *40*, 679-694.
71. Cosconati, S. F., Stefano; Perryman, Alex L; Harris, Rodney; Goodsell, David S; Olson, Arthur J. (2010) Virtual screening with AutoDock: theory and practice, *Expert opinion on drug discovery* *5*, 597-607.
72. Ajoy Kumer; Md Wahab Khan. (2021) Synthesis, characterization, antimicrobial activity and computational exploitations of ortho toluidinium carboxylate ionic liquids, *Journal of Molecular Structure* *1245*, 131087; <https://doi.org/131010.131016/j.molstruc.132021.131087>.
73. Hoque, M. M. H., Md Sajib; Kumer, Ajoy; Khan, Md Wahab;. (2020) Synthesis of 5, 6-diaroylisoindoline-1, 3-dione and computational approaches for investigation on structural and mechanistic insights by DFT, *Molecular Simulation* *36*, 1298-1307; <https://doi.org/1210.1080/08927022.08922020.01811866>.
74. Kumer, A., and Khan, M. W. (2021) The effect of alkyl chain and electronegative atoms in anion on biological activity of anilinium carboxylate bioactive ionic liquids and computational approaches by DFT functional and molecular docking, *Heliyon*, e07509.
75. Nahar, L. A., Kumer, A., and Khan, M. W. (2021) Investigation of catalytic effect on carbon-carbon bond formation by Baylis-Hillman (BH) reaction between (2/3/4)-nitro-arylaldehyde and alkylacrylates and computational approaches through DFT functional, *Heliyon*, e08139.
76. Nath, A., ; Kumer , Ajoy , ; Md, Wahab Khan;. (2020) Synthesis, computational and molecular docking study of some 2, 3-dihydrobenzofuran and its derivatives, *Journal of Molecular Structure* *1224*, 129-225. <https://doi.org/110.1016/j.molstruc.2020.129225>.
77. Nath, A., Kumer, A., Zaben, F., and Khan, M. W. (2021) Investigating the binding affinity, molecular dynamics, and ADMET properties of 2, 3-dihydrobenzofuran derivatives as an inhibitor of fungi, bacteria, and virus protein, *Beni-Suef University Journal of Basic and Applied Sciences* *10*, 1-13.

78. Hoque, M. M., ; Ajoy, Kumer; Hussien, Md. Sajib; Khan, Md Wahab;. (2021) Theoretical Evaluation of 5, 6-Diaroylisoindoline-1,3-dione as Potential Carcinogenic Kinase PAK1 Inhibitor: DFT Calculation, Molecular Docking Study and ADMET Prediction, *International journal of Advanced Biological and Biomedical Research* 9, 77-104; 110.22034/IJABBR.22021.45696.
79. Salentin, S., Haupt, V. J., Daminelli, S., and Schroeder, M. (2014) Polypharmacology rescored: Protein–ligand interaction profiles for remote binding site similarity assessment, *Progress in biophysics and molecular biology* 116, 174-186.
80. Hollingsworth, S. A., and Dror, R. O. (2018) Molecular dynamics simulation for all, *Neuron* 99, 1129-1143.
81. Strovel, J., Sittampalam, S., Coussens, N. P., Hughes, M., Inglese, J., Kurtz, A., Andalibi, A., Patton, L., Austin, C., and Baltezor, M. (2016) Early drug discovery and development guidelines: for academic researchers, collaborators, and start-up companies, *Assay Guidance Manual [Internet]*.
82. Pellegatti, M. J. E. o. o. d. m., and toxicology. (2012) Preclinical in vivo ADME studies in drug development: a critical review, 8, 161-172.
83. Li, A. P. J. D. d. t. (2001) Screening for human ADME/Tox drug properties in drug discovery, 6, 357-366.
84. Yang, Y., Zhao, Y., Yu, A., Sun, D., and Yu, L. (2017) Oral drug absorption: Evaluation and prediction. In *Developing solid oral dosage forms*, pp 331-354, Elsevier.
85. Onetto, A. J., and Sharif, S. J. S. (2021) Drug Distribution.
86. Zhang, Z., and Tang, W. J. A. P. S. B. (2018) Drug metabolism in drug discovery and development, 8, 721-732.
87. Currie, G. M. J. J. o. n. m. t. (2018) Pharmacology, part 2: introduction to pharmacokinetics, 46, 221-230.
88. Guengerich, F. P. J. D. m., and pharmacokinetics. (2010) Mechanisms of drug toxicity and relevance to pharmaceutical development, 1010210090-1010210090.
89. Verma, J., Khedkar, V. M., and Coutinho, E. C. (2010) 3D-QSAR in drug design-a review, *Current topics in medicinal chemistry* 10, 95-115.
90. Scrocco, E., and Tomasi, J. (1973) The electrostatic molecular potential as a tool for the interpretation of molecular properties, In *New concepts II*, pp 95-170, Springer.
91. Politzer, P., and Truhlar, D. G. (2013) *Chemical applications of atomic and molecular electrostatic potentials: reactivity, structure, scattering, and energetics of organic, inorganic, and biological systems*, Springer Science & Business Media.
92. Müller, J. J., Lapko, A., Ruckpaul, K., and Heinemann, U. (2002) Modeling of electrostatic recognition processes in the mammalian mitochondrial steroid hydroxylase system, *Biophysical chemistry* 100, 281-292.